

Research Paper

Targeting of Magnetic Nanoparticle-coated Microbubbles to the Vascular Wall Empowers Site-specific Lentiviral Gene Delivery *in vivo*

Yvonn Heun^{1,10}, Staffan Hildebrand², Alexandra Heidsieck³, Bernhard Gleich³, Martina Anton⁴, Joachim Pircher^{7,8}, Andrea Ribeiro⁸, Olga Mykhaïlyk⁴, Dietmar Eberbeck⁵, Daniela Wenzel⁶, Alexander Pfeifer², Markus Woernle⁸, Florian Krötz⁹, Ulrich Pohl^{1,10,11}, Hanna Mannell^{1,10}✉

1. Walter Brendel Centre of Experimental Medicine, BMC, Ludwig-Maximilians-University, Großhaderner Str. 9, 82152 Planegg, Germany.
2. Institute of Pharmacology and Toxicology, Biomedical Center University of Bonn, Sigmund-Freud-Strasse 25, 53105 Bonn, Germany.
3. Central Institute of Medical Engineering (IMETUM), Technical University Munich, Boltzmannstrasse 11, 85748 Garching, Germany.
4. Institute of Experimental Oncology and Therapy Research, Technical University Munich, Ismaninger Strasse 22, 81675 Munich, Germany.
5. Physikalisch-Technische Bundesanstalt, Abbestr. 2-12, 10587 Berlin, Germany.
6. Institute of Physiology I, Life&Brain Center, University Clinic Bonn, 53127 Bonn.
7. Medizinische Klinik und Poliklinik I, Klinikum der Universität München, Marchioninistrasse 15, 81377 Munich, Germany.
8. Medizinische Klinik und Poliklinik IV, Klinikum der Universität München, Ziemssenstrasse 1, 80336 Munich, Germany.
9. Invasive Cardiology, Starnberg Community Hospital, Osswaldstrasse 1, 82319 Starnberg, Germany.
10. DZHK (German Center for Cardiovascular Research) partner site Munich Heart Alliance, Munich.
11. Munich cluster for systems neurology, (SyNergy) Munich.

✉ Corresponding author: Dr. Hanna Mannell, Walter Brendel Centre of Experimental Medicine, BMC, Ludwig-Maximilians-University, Großhaderner Str. 9, 82152 Planegg, Germany. Tel: + 49 89 218071519, Fax: +49 89 218071553, Email: hanna.mannell@lrz.uni-muenchen.de

© Ivyspring International Publisher. Reproduction is permitted for personal, noncommercial use, provided that the article is in whole, unmodified, and properly cited. See <http://ivyspring.com/terms> for terms and conditions.

Received: 2016.05.17; Accepted: 2016.09.13; Published: 2017.01.01

Abstract

In the field of vascular gene therapy, targeting systems are promising advancements to improve site-specificity of gene delivery. Here, we studied whether incorporation of magnetic nanoparticles (MNP) with different magnetic properties into ultrasound sensitive microbubbles may represent an efficient way to enable gene targeting in the vascular system after systemic application. Thus, we associated novel silicon oxide-coated magnetic nanoparticle containing microbubbles (SO-Mag MMB) with lentiviral particles carrying therapeutic genes and determined their physico-chemical as well as biological properties compared to MMB coated with polyethylenimine-coated magnetic nanoparticles (PEI-Mag MMB). While there were no differences between both MMB types concerning size and lentivirus binding, SO-Mag MMB exhibited superior characteristics regarding magnetic moment, magnetizability as well as transduction efficiency under static and flow conditions *in vitro*. Focal disruption of lentiviral SO-Mag MMB by ultrasound within isolated vessels exposed to an external magnetic field decisively improved localized VEGF expression in aortic endothelium *ex vivo* and enhanced the angiogenic response. Using the same system *in vivo*, we achieved a highly effective, site-specific lentiviral transgene expression in microvessels of the mouse dorsal skin after arterial injection. Thus, we established a novel lentiviral MMB technique, which has great potential towards site-directed vascular gene therapy.

Key words: lentiviral gene delivery, magnetic targeting, ultrasound, magnetic microbubbles, VEGF, endothelial cells.

Introduction

Gene therapy constitutes a promising way to specifically modulate signalling pathways and vascular physiological responses in both research and medical therapy. Regarding the vasculature,

therapeutic options comprise local treatment of ischemia and tumors or organ specific therapy for treatment of diabetic retinopathy, to mention a few. However, an effective therapeutic approach, which

combines high efficiency and site-specificity following intravascular application, is still not available. Although the vascular system represents an ideal route to deliver therapeutic genes, it is associated with systemic distribution and thus non-specific delivery of the therapeutic vectors resulting in undesired side-effects. Furthermore, biological interactions and clearance mechanisms contribute to low gene transfer efficiency. Therefore, the application of a carrier system capable of improving circulation time in combination with specific targeting of the carriers is an essential prerequisite for the development of safe and efficient gene therapy. Microbubbles (MB) have been applied as contrast agent in diagnostic ultrasound imaging since three decades¹. Due to their unique physico-chemical properties, they are in addition used as carriers for biomaterials^{2,3}. The gas-filled MB not only allow for controlled and localized substance release following local sonication, but in addition feature high shape flexibility important for the passage through the microcirculation in order to decrease clearance of the bound substance^{3,4}. However, systemic distribution and hence dilution of the MB strongly hampers the benefits given by this approach. Therefore, targeting mechanisms combining local MB disruption with site-specific MB trapping are under intense investigations^{5,6}. One such approach is the coating of MB with magnetic nanoparticles (MNP). The resulting magnetic microbubbles (MMB) represent an innovative and unique gene carrier system enabling localized magnetic accumulation of genetic vectors at the site of magnetic field (MF) exposure with simultaneous vector release and gene transfer induced by sonication. In previous work from our group we used MNP for targeted transfer of oligonucleotides to primary endothelial cells^{7,8} and recently we generated MMB and successfully proved their functionality as guidable carrier system for pDNA *in vivo*⁹. To further improve gene transfer efficiency and transgene expression we established lentiviral MMB in a previous *in vitro* study¹⁰. Although we could prove the feasibility of this approach, further optimization of the lentiviral MMB technique was shown to be necessary, particularly with regard to higher magnetizability to allow for successful therapeutic application *in vivo*.

Vascular endothelial growth factor (VEGF) is considered a therapeutic gene, since it is the most potent angiogenic factor with unique actions on vascular endothelium¹¹. Besides its important physiological role during embryonic development and wound healing, it is substantially involved in processes regulating adaptive angiogenic responses to ischemia and the development of diabetic retinopathy

and tumor vascularization¹¹. Hence, VEGF has been used as a therapeutic target either to promote vascularization by its induction^{12,13} or to impair vessel growth by its inhibition¹⁴. An intravascular targeting strategy, such as the lentiviral MMB technique, may constitute a valuable tool to achieve tissue specific angiogenic therapy by targeted gene delivery of VEGF.

In this study, we thus evaluated a new type of lentiviral MMB containing silicon oxide-coated MNP (SO-Mag) with enhanced performance compared to our former established PEI-Mag MMB^{9,10} in terms of physico-chemical properties and gene transfer efficiency under static as well as flow conditions. Furthermore, we aimed to study whether our targeting system would be efficient to locally deliver genes to aortic endothelium *ex vivo* and to the microcirculation of mice *in vivo* upon systemic application.

Results

Characterization of lentiviral SO-Mag and PEI-Mag magnetic nanoparticle-coated microbubbles.

Magnetic microbubbles were generated by coating lipid microbubbles with SO-Mag magnetic nanoparticles. The physico-chemical properties of these MMB, important for successful targeting *in vivo*, were determined and compared to microbubbles coated with PEI-Mag magnetic nanoparticles^{9,10}. As shown in Table 1, the mean diameter of the MMB increased after integration of SO-Mag MNP and association of lentivirus reduced the diameter of the MMB compared to naked MB (*p<0.05, n=3). However, no difference between PEI-Mag and SO-Mag MMB could be detected (Table 1; *p<0.05, n=3). Despite the fact that SO-Mag and PEI-Mag MNP possess opposed ζ potentials (-16.1 ± 0.6 mV and $+14.7 \pm 1.2$ mV, respectively) the resulting MMB types both exhibit a positive ζ potential. Calculations of the average number of MNP embedded in one MMB revealed that lentiviral SO-Mag MMB contain significantly more MNP compared to lentiviral PEI-Mag MMB (Table 1; *p<0.05, n=3). To prove the ability of the SO-Mag MMB to adequately bind lentivirus, fluorescently labelled lentiviral particles (pCHIV.eGFP) were incubated with the MMB. Flow cytometry analysis revealed a complete association between MMB and pCHIV.eGFP lentiviral particles. However, no difference in lentivirus binding between SO-Mag MMB and PEI-Mag MMB was detected (Figs. 1a and b; *p<0.05, n=4). To further assess the lentivirus binding capacity of MMB and their magnetizability, MMB coated with a GFP-expressing

lentivirus were separated from the solution by application of a MF. The resulting concentrated MMB and the MMB-free supernatant were separately applied to primary human umbilical vein endothelial cells (HUVEC) following simultaneous US and MF exposure (Fig. 1c). The low GFP expression in cells exposed to MMB-free supernatants clearly demonstrated the almost complete association of lentivirus from the solution to both MMB compositions. However, if the magnetically concentrated MMB were targeted to cells, SO-Mag MMB yielded a significantly higher transduction

efficiency compared to PEI-Mag MMB (*p<0.05, n=3 in duplicates). This may be explained by the finding that SO-Mag MMB exhibited a higher velocity under a magnetic field compared to PEI-Mag MMB (19.10 ± 0.69 μm/s vs. 11.40 ± 0.22 fA m², respectively; Fig. 1d). This difference in magnetic potency became even more striking by calculation of the magnetic moments of the two MMB types, with SO-Mag MMB possessing an about three-fold higher magnetic moment than the PEI-Mag MMB (94.74 ± 0.47 fA m² vs. 32.14 ± 0.12 fA m², respectively; Fig. 1e).

TABLE 1. Physical characteristics of MB with or without associated MNP (150 Fe μg/ml) or LV (5*10⁸ VP/ml MMB).

	LV	Diameter [μm] ^{a, b}	μg Fe/MMB ^b	MNP/MMB ^{b, c}	ζ Potential [mV] ^b
naked MB	-	5.0 ± 0.2	-	-	6.2 ± 0.3
pCHIV.eGFP	+	1.9 *10 ⁻¹ ± 0.8 *10 ⁻²	-	-	-8.8 ± 0.6
SO-Mag MNP	-	4.0*10 ⁻² ± 1.4*10 ^{-3d}	-	-	-16.1 ± 0.6
SO-Mag MMB	-	6.1 ± 0.1 *	2.0*10 ⁻⁸ ± 8.1*10 ⁻¹¹	3.6*10 ⁶ ± 2.5*10 ⁻⁴	3.9 ± 0.5
	+	4.9 ± 0.5	4.4*10 ⁻⁸ ± 8.1*10 ⁻⁹	6.2*10 ⁶ ± 1.2*10 ⁻⁶ #	5.0 ± 0.2
PEI-Mag MNP	-	2.8*10 ⁻² ± 0.2*10 ^{-2d}	-	-	14.7 ± 1.2
PEI-Mag MMB	-	5.6 ± 0.2 *	2.5*10 ⁻⁸ ± 1.5*10 ⁻⁹	1.7*10 ⁶ ± 4.6*10 ⁻⁴	9.6 ± 0.5
	+	4.7 ± 0.2	6.8*10 ⁻⁸ ± 7.4*10 ⁻⁹	3.4*10 ⁶ ± 2.4*10 ⁻⁵ #	9.4 ± 0.5

^a Particle diameter for MMB and lentivirus-MMB complexes, hydrodynamic diameter for sole pCHIV.eGFP LV; ^b Mean ± SEM; *p<0.05 vs. naked MB, #p<0.05 vs. MB+MNP, n=3 in duplicates; ^c MNP iron/particle content: 6.2*10⁻¹³ μg Fe/SO-Mag MNP and 1.4*10⁻¹² μg Fe/PEI-Mag MNP; ^d adapted from Almstätter et al.¹⁵ MNP: magnetic nanoparticles; MMB: magnetic microbubble; MB: microbubble; LV: lentivirus; Fe: iron.

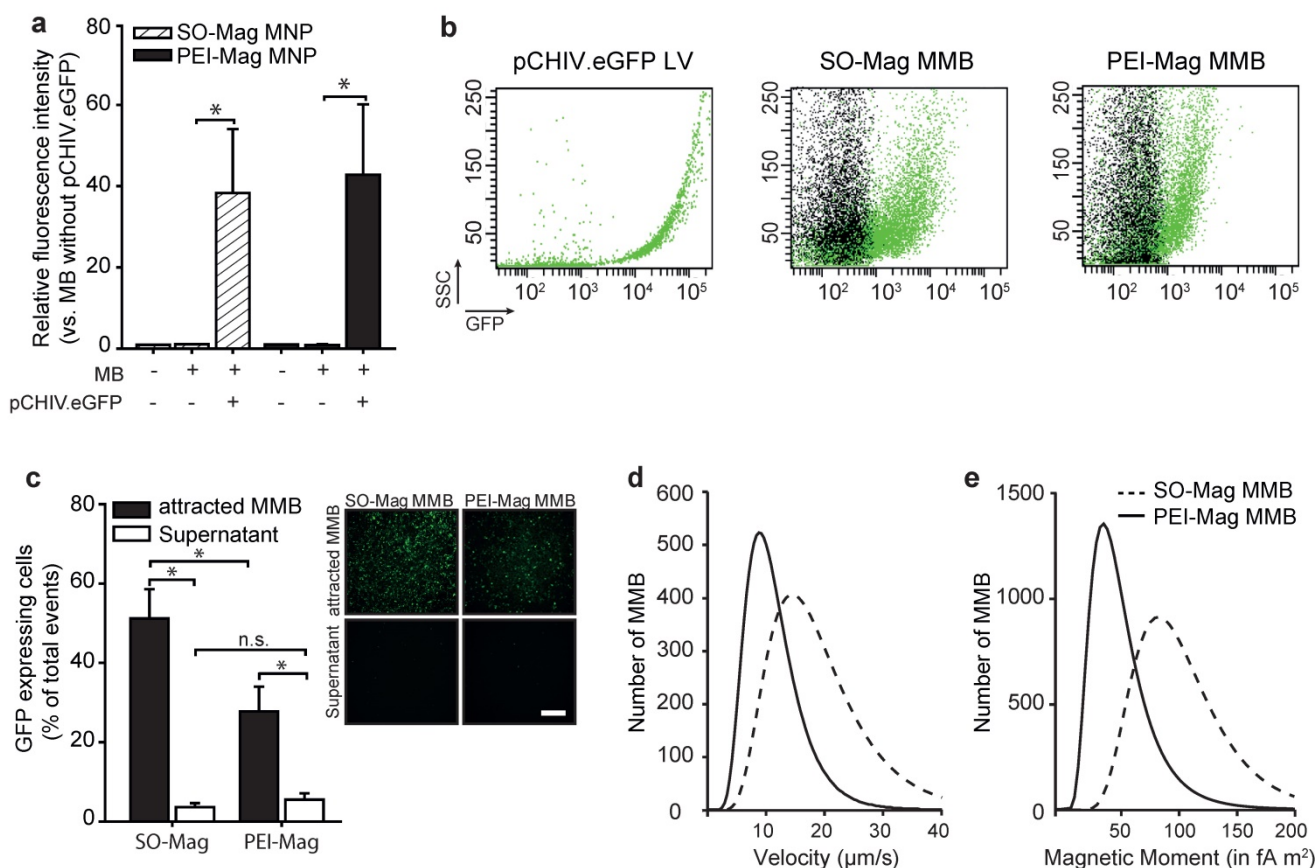


Figure 1. Characterization of MB containing SO-Mag or PEI-Mag MNP. (a) Lentivirus (3*10⁸ VP/100 μl MMB) binding to MMB was quantified by flow cytometry (mean ± SEM; *p<0.05, n=3). (b) Representative dot plots of lentiviral pCHIV.eGFP particles and MMB solutions without (black) or with (green) associated lentivirus as assessed by flow cytometry. (c) Magnetizability of SO-Mag and PEI-Mag MMB coupled to GFP-lentivirus (1.5*10⁸ VP/100 μl MMB) was assessed by exposing solutions to an external MF for 15 min with subsequent application of MMB-free supernatant and concentrated MMB to endothelial cell culture. Transduction rates (percentage of GFP expressing cells) were assessed by flow cytometry 72 h later (mean ± SEM; *p<0.05, n=6). Panels show representative fluorescence images of GFP expression in cells. Scale bar indicates 500 μm. (d) Velocity measurements and (e) calculated magnetic moments of SO-Mag and PEI-Mag MMB solutions (150 μg Fe/ml). MB: microbubble, MMB: magnetic microbubble, LV: lentivirus, SSC: side scatter.

Lentiviral SO-Mag MMB increase endothelial gene delivery by a caveolin-dependent endocytic mechanism

To evaluate gene transfer efficiencies of SO-Mag MMB in dependence of the different technical parameters MF and US, SO-Mag MMB coated with a GFP expressing lentivirus were added to endothelial cell cultures following application of either a MF or US or combined treatment. Flow cytometry analysis of GFP expressing cells revealed that application of lentiviral SO-Mag MMB with US alone did not enhance transduction efficiency compared to sole lentiviral SO-Mag MMB application (Figs. 2a and b). In contrast, exposure to a MF resulted in a strong increase in transduction efficiency of SO-Mag lentiviral MMB (* $p \leq 0.05$, $n=4$). A cumulative effect of combined MF and US exposure after lentiviral SO-Mag MMB application on transduction efficiency could be observed compared to sole lentiviral SO-Mag MMB application (* $p \leq 0.05$, $n=4$). Although the same pattern was observed with PEI-Mag MMB, SO-Mag MMB possessed a significantly higher potency to deliver the GFP expressing lentivirus to endothelial cells in the combined setting (* $p \leq 0.05$, $n=4$). To identify the responsible mechanism of uptake relevant for lentiviral SO-Mag MMB-mediated gene delivery to endothelial cells, cells were treated with inhibitors of different endocytic pathways previous to SO-Mag MMB mediated transduction. Inhibition of caveolae-mediated endocytosis by methyl- β -cyclodextrin (M β CD), which extracts cholesterol from the plasma membrane^{16,17}, was thereby shown to significantly decrease lentiviral uptake compared to cells without inhibitor treatment (Fig. 2c; * $p \leq 0.05$, $n=5$ in duplicates). In contrast, inhibition of phagosome-lysosome fusion by ammoniumchloride (NH₄Cl)¹⁸ or inhibition of the clathrin-mediated endocytic pathway by cytochalasin B (CytoB)¹⁶ did not influence lentiviral SO-Mag MMB-mediated transduction (** $p \leq 0.05$, $n=5$ in duplicates).

SO-Mag MMB improve targeted lentiviral gene delivery to vessels under flow conditions

To evaluate the performance of the lentiviral MMB technique under flow conditions, endothelial cells cultured in channel slides were perfused with MMB coupled to a luciferase reporter lentivirus with simultaneous application of MF and US. As seen in Figure 3a, lentiviral MMB-mediated gene transfer under a shear rate of 1 dyn/cm² resulted in a strong and local luciferase expression regardless of MNP type. However, the lentiviral PEI-Mag MMB showed reduced transduction efficiencies at increased shear

rates of 5 and 7.5 dyn/cm², whereas the lentiviral SO-Mag MMB mediated transgene expression remained high under these conditions (* $p \leq 0.05$, ** $p \leq 0.01$, $n=4$). Thereby, absence of US treatment significantly hampered luciferase expression compared to full treatment as seen in Figure 3b. Importantly, if only US without MF was applied, transgene expression was minimal, emphasizing the importance of magnetic attraction under flow conditions for successful gene delivery (* $p \leq 0.01$, $n=4$). Additionally, the use of lentivirus-MNP complexes without MB resulted in insufficient gene transfer (Fig. 3c; * $p \leq 0.05$, ** $p \leq 0.01$, $n=4$). Thus, as the SO-Mag MMB were repeatedly found to possess functional advantages over PEI-Mag MMB, only these MMB were used in further experiments. In intact aortic segments we analysed the ability of the lentiviral MMB technique to locally transduce complete vessels under flow conditions using SO-Mag MMB carrying GFP expressing lentivirus and a recirculation setting at a mean shear rate of 7-8 dyn/cm², while MF and US were locally applied as depicted in Figure 3d. The resulting GFP expression was essentially localized in the region of MF and US application, as visualized by fluorescence microscopy of the whole aorta 72h after transduction (Fig. 3e). In aortas without MF and US targeting no transgene expression could be detected. Specific gene transfer to the endothelial cell layer could be verified by PECAM-1 co-staining of GFP expressing cells in cross sections of the treated aortas (Fig. 3f). GFP expression was thereby uniquely found in endothelial cells and not in other cell types of the vascular wall, such as vascular smooth muscle cells.

LV-MMB mediated targeted gene delivery of VEGF to vessels enhances angiogenesis

To test if the LV-MMB technique has potential for therapeutic use, we investigated whether SO-Mag MMB mediated targeted delivery of a lentiviral human (hu) VEGF expression vector to the endothelium of vessels has the ability to enhance vessel sprouting. Targeting of aortic endothelium was performed under flow using SO-Mag MMB coated with either huVEGF lentivirus or GFP lentivirus (huVEGF-MMB or GFP-MMB, respectively) by simultaneous application of a MF and US (see Fig. 3d). Aortas targeted with lentiviral huVEGF-MMB expressed high levels of human VEGF compared to aortas targeted with GFP-MMB as control (Fig. 4a; ** $p \leq 0.01$, $n=6$). In addition, a 6-fold increase in secreted human VEGF was found in the supernatants of aortas targeted with lentiviral VEGF-MMB compared to GFP-MMB (Fig. 4b; * $p \leq 0.05$, $n=6$).

Finally, targeted delivery of lentiviral VEGF-MMB enhanced the number of aortic vessel sprouts as well as the vessel sprouting area compared to targeted

delivery of lentiviral GFP-MMB (* $p \leq 0.05$, $n=6$ aortas with 4 rings each, Fig. 4c-e).

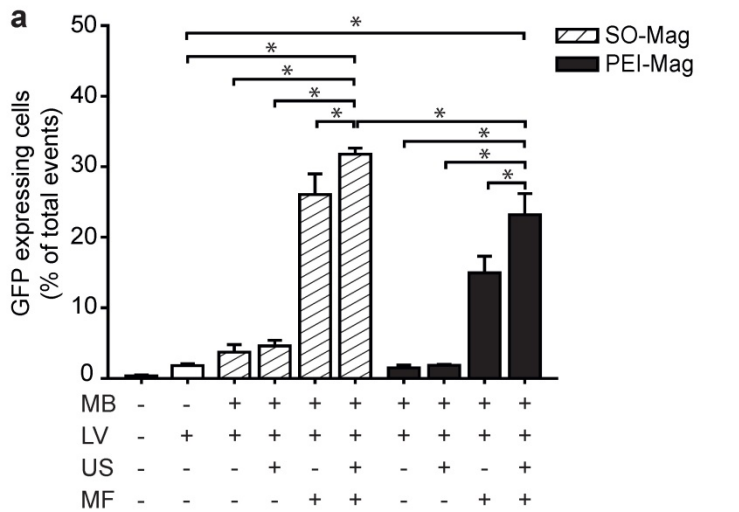
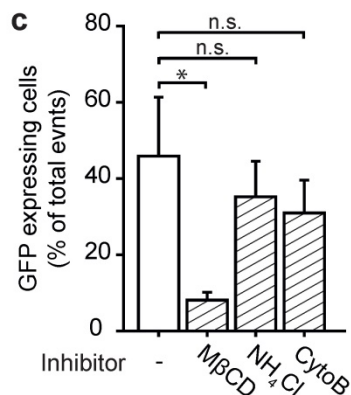
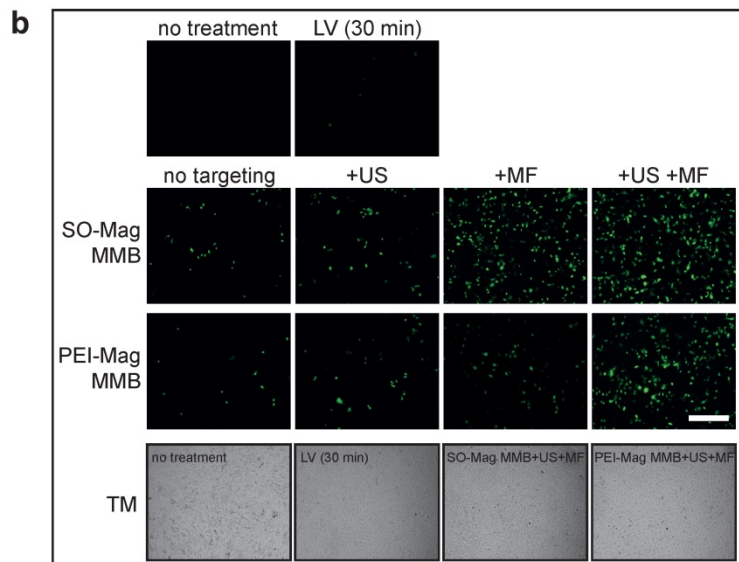


Figure 2. Biological properties of SO-Mag and PEI-Mag MMB *in vitro*. (a) Gene transfer efficiency of the lentiviral MMB technique using the two MMB types was assessed by MMB mediated transduction of endothelial cell culture. Single and combined parameters of the technique (GFP-lentivirus \pm PEI-Mag/SO-Mag MMB \pm MF \pm US) were applied and transduction efficiencies were assessed by flow cytometry 72 h later (mean \pm SEM; * $p \leq 0.05$ to full treatment with SO-Mag MMB, $n=4$ in duplicates). (b) Representative fluorescence images of GFP expression in cells. Lower panels: representative transmission (TM) light pictures. Scale bar indicates 500 μm . (c) Putative cellular uptake mechanisms underlying the lentiviral MMB technique were analysed by inhibiting caveolin-dependent endocytosis (Methyl- β -cyclodextrin, M β CD; 10 mM), endosome-lysosome fusion (Ammoniumchloride, NH $_4$ Cl; 10 nM) or clathrin-dependent endocytosis (CytochalasinB, CytoB; 10 μM) prior to the application of the MMB technique and flow cytometry analysis of GFP expressing cells (mean \pm SEM; * $p \leq 0.05$, $n=4$). MMB: magnetic microbubble, LV: lentivirus, US: ultrasound, MF: magnetic field.



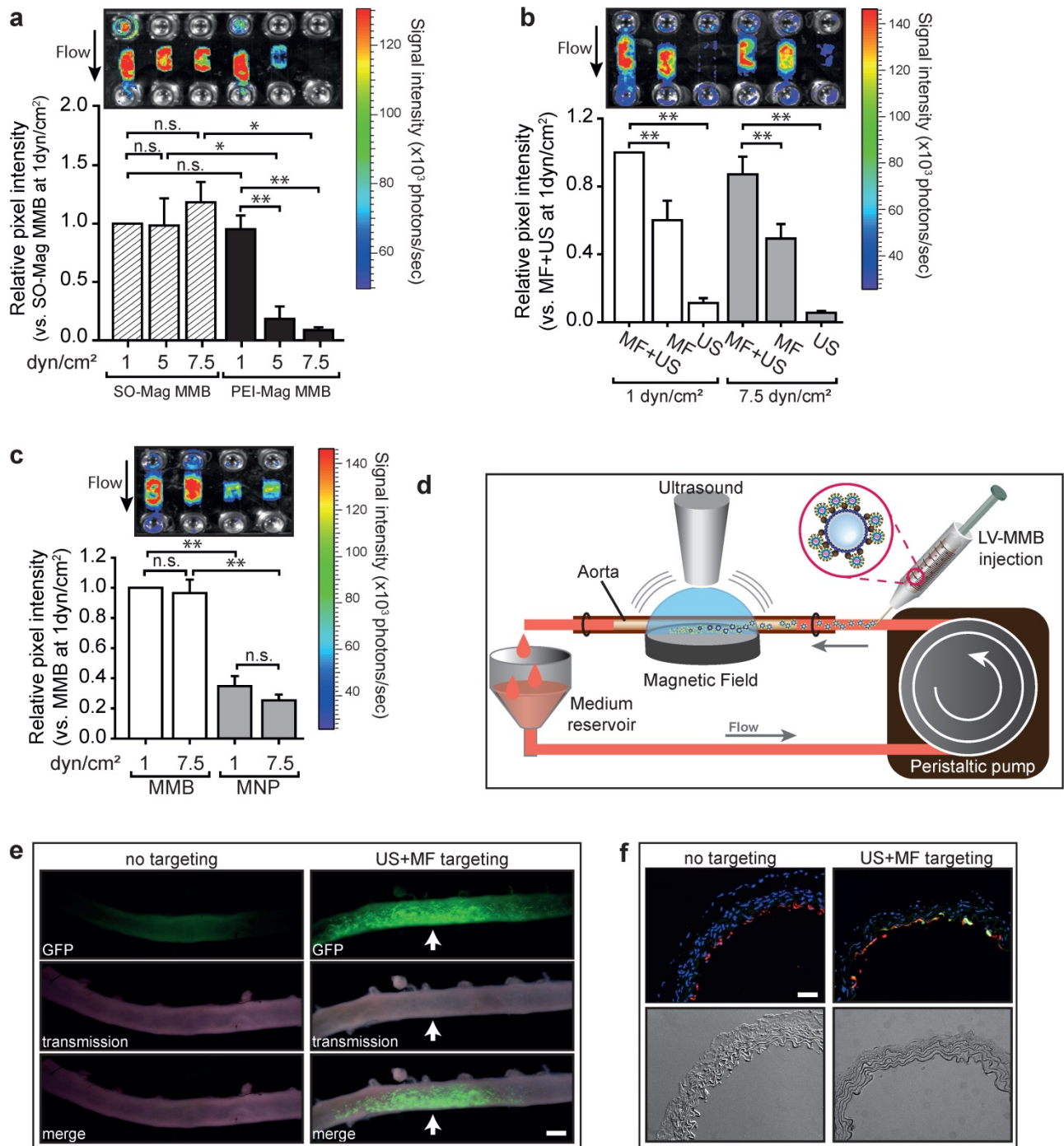


Figure 3. Targeted transduction of aortic endothelium under flow using lentiviral SO-Mag MMB. Gene transfer efficiency under flow was assessed (a) with SO-Mag and PEI-Mag MMB carrying luciferase expressing lentivirus under different shear rates (1, 5 and 7.5 dyn/cm²), (b) with and without MF and US targeting and (c) with lentiviral SO-Mag MNP complexes. Graphs show quantification of luciferase activity (mean \pm SEM; * p < 0.05, n = 4). Upper panels show representative bioluminescence images. (d) Schematic illustration of the MMB transduction setting applied to mouse aortas. SO-Mag MMB coated with GFP expressing lentivirus were added into a recirculation system applying a shear stress of around 7-8 dyn/cm². Simultaneously, US and MF were applied to locally accumulate and destroy the lentiviral MMB. (e) GFP expression in mouse aortas after SO-Mag MMB mediated lentiviral transduction with (right panels) and without (left panels) MF and US targeting was assessed by fluorescence microscopy of the whole aortas (n = 3). Arrow indicates site of MF and US application. Scale bar indicates 1 mm. (f) Specific targeting of endothelial cells in aortas was verified by immunofluorescence staining of cross-sectional slices (n = 3). Red: PECAM-1, green: GFP expression, blue: Hoechst nuclear stain. Scale bar indicates 10 μ m. MMB: magnetic microbubble, LV: lentivirus, MF: magnetic field, US: ultrasound.

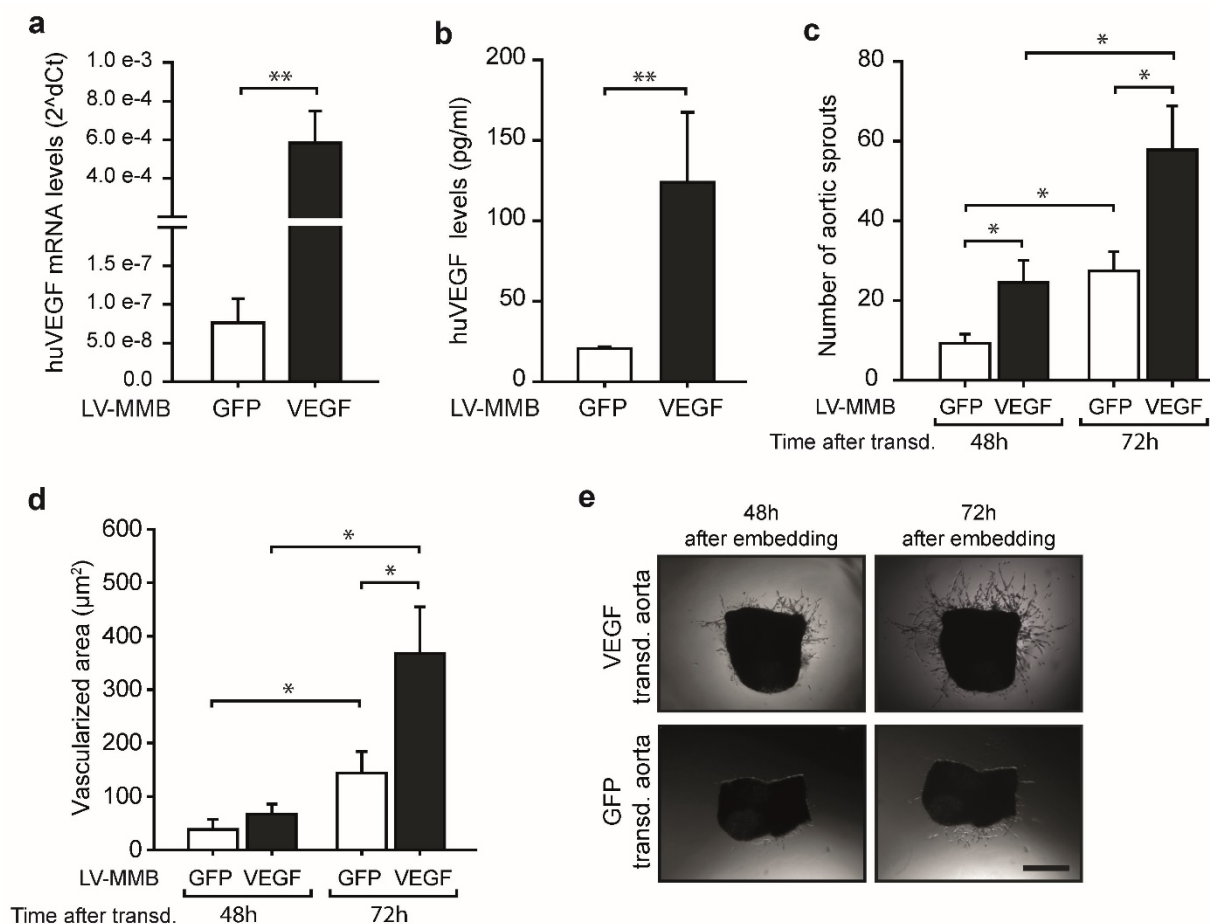


Figure 4. SO-Mag MMB mediated lentiviral delivery of VEGF to vessels enhances angiogenesis. (a) SO-Mag MMB mediated targeting of huVEGF expressing lentivirus in mouse aortic endothelium *ex vivo* resulted in strong mRNA expression of huVEGF, as measured by qRT-PCR (mean \pm SEM; ** $p \leq 0.01$, $n=6$, house-keeping gene: murine 18S rRNA) and (b) enhanced secretion of huVEGF into the supernatant of these aortas, as assessed by ELISA, compared to GFP transduced aortas (mean \pm SEM; ** $p \leq 0.01$, $n=6$). As a result, an increased number of aortic sprouts (c) and a larger vascularized area around the aortic rings (d) was detected in VEGF transduced aortas compared to GFP transduced ones (mean \pm SEM; * $p \leq 0.05$, $n=6$ aortas with 4 rings each). (e) Representative images of aortic rings expressing huVEGF or GFP by SO-Mag MMB mediated lentiviral gene delivery. Scale bar indicates 200 μm .

Targeted lentiviral gene delivery *in vivo* upon systemic application of SO-Mag MMB

To investigate if the lentiviral MMB technique is indeed applicable for *in vivo* gene targeting, SO-Mag MMB coated with luciferase expressing lentivirus were injected into the carotid artery of C57BL/6 wild type mice carrying a dorsal skinfold chamber (DSFC)¹⁹. Targeting of the lentiviral MMB to microvessels of the dorsal skin was accomplished by simultaneous application of a MF and US positioned on opposite sides of the DSFC window (see Fig. 5a). Eight days after lentiviral MMB targeting *in vivo*, mice showed a strong and local bioluminescence signal at the area of MF and US exposure (DSFC window) demonstrating successful delivery of the luciferase expressing lentivirus via SO-Mag MMB targeting (Fig. 5b; $n=3$). Lentiviral MMB injection without MF and US targeting, in contrast, did not result in an expression signal in the DSFC (Fig. 5b; $n=3$). Moreover, the number of integrated provirus copies in genomic

DNA was significantly higher in the dorsal skin of mice receiving MF and US treatment upon injection of lentiviral SO-Mag MMB compared to dorsal skins of mice only receiving lentiviral SO-Mag MMB (Fig. 5c, $p < 0.05$, $n=3$). Measurements of the MNP distribution in different organs 1 hour after MMB injection revealed the highest accumulation in the lungs and the liver (Fig. 5d; $n=5$). 96h after MMB injection, however, no MNPs could be detected indicating a clearance from the system and/or integration into the iron metabolism ($n=4$). As the lungs and the liver were identified as the major sites of MNP accumulation, these organs were also screened for integrated lentivirus copies. As seen in figure 5e, integrated provirus was also detected in the lungs and liver in mice receiving MF and US to the dorsal skin upon injection of SO-Mag MMB but to a significantly lower level compared to the dorsal skin ($p < 0.05$, $n=3-4$). Importantly, whereas lentiviral MMB treatment without MF and US targeting caused relatively strong transgene expression in the lung and

liver, targeting with MF and US to the dorsal skin upon lentiviral MMB injection reduced the transgene

expression in the lungs (Fig. 5f, $p=0.057$, $n=3$) and liver (Fig. 5f, $p<0.05$, $n=4$).

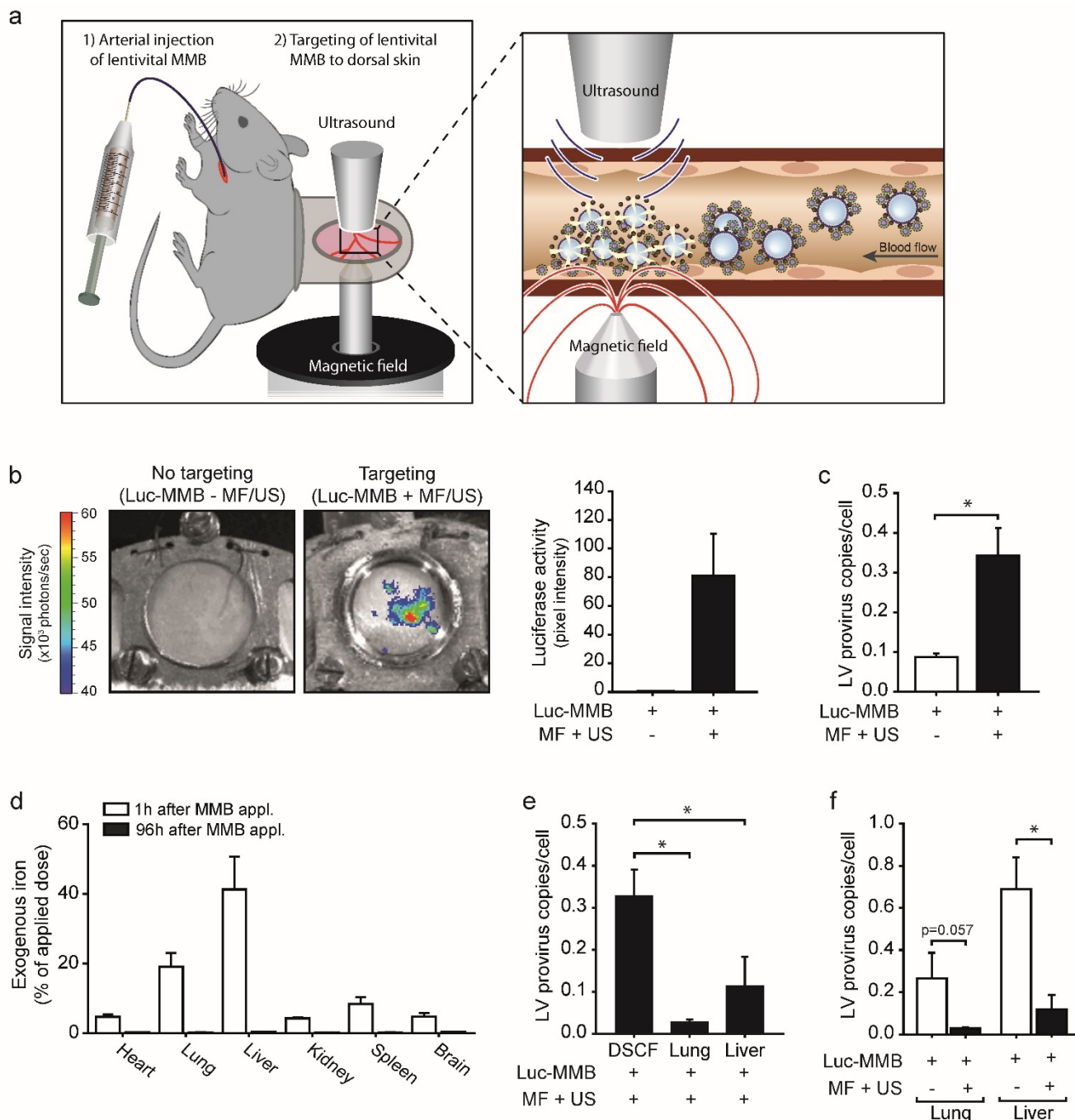


Figure 5. SO-Mag MMB achieve targeted lentiviral delivery after systemic injection *in vivo*. (a) Schematic illustration of the *in vivo* setting applied for lentiviral MMB mediated gene delivery to the mouse dorsal skin. Left image: The observation window of the DSFC was centred between the tip of an electromagnet and the US transducer. MF and US were applied simultaneous to lentiviral MMB injection via the Arteria carotis catheter to achieve localized gene delivery. Right image: Intravascular lentiviral MMB accumulate at the site of MF and disrupt upon US application within the vessel. The triggered release of the lentiviral cargo results in enhanced local gene transfer to endothelial cells. (b) Representative bioluminescence images of the dorsal skinfold chamber in mice treated with luciferase expressing lentivirus coupled to MMB 8 days after application. Treatment with lentiviral MMB without targeting did not result in any transgene expression i.e. luciferase activity in the dorsal skin (left image), whereas targeted treatment with lentiviral MMB resulted in local luciferase activity in the targeted dorsal skin (right image). Bars next to images show quantification of bioluminescence signals (luciferase activity) in mice treated with lentiviral SO-Mag MMB with or without magnetic and ultrasound targeting ($n=3$). (c) Genomic provirus copy numbers/cell was higher in the dorsal skin of mice treated with MF and US after systemic injection of lentiviral SO-Mag MMB compared to no targeting ($*p<0.05$, $n=3$). (d) The MNP amount in different tissues was assessed using MPS 1h and 96h after injection respectively ($n=5$). (e) Integrated provirus copies/cell were in addition detected in lung and liver of mice receiving MF and US targeting to the dorsal skin but significantly less compared to the targeted dorsal skin ($*p<0.05$, $n=3-4$). (f) MF and US exposure after SO-Mag MMB injection reduced the transduction of secondary sites (lung and liver) compared to no targeting ($*p<0.05$, $n=4$). MMB: Magnetic microbubbles, MF: Magnetic Field, US: Ultrasound, DSFC: dorsal skinfold chamber.

Discussion

This study demonstrates that the lentiviral MMB technique improves site-directed vascular gene targeting to isolated vessels and to a vascular bed *in vivo*. For the first time, ultrasonic microbubble-mediated delivery^{1,3} and a magnetic nanoparticle (MNP)-assisted transport system^{20,21} were combined with lentiviral gene delivery successfully generating a potent site-specific gene transfer system for *in vivo* applications.

The use of MNP in combination with various genetic vectors (magnetofection method) has been object of several *in vitro* and *in vivo* studies by us^{7,8,22,23} and other groups^{15,24,25}. However, gene targeting by MNP, especially after systemic administration *in vivo*, has proven to be insufficient probably due to low magnetic moments of the single MNP, particle aggregation in the blood, and rapid clearance from the circulation. The embedding of several MNP within the lipid monolayer of a MB, as studied here, has not only the advantage to reduce their biological clearance but also enormously increases the ability of site-specific targeting due to the increased magnetic moment of the MMB, which enables the MMB to withstand the forces of blood flow. Indeed, our single SO-Mag MMB exhibited a higher magnetic moment compared to the single SO-Mag MNP, which resulted in higher transduction efficiency under flow conditions. These data clearly demonstrate the superior magnetic properties of SO-Mag MMB as well as the supremacy of MMB over MNP-lentivirus complexes.

The choice of the genetic vector with which a targeting system is combined is an important factor determining the success of the therapeutic intervention. Lentiviruses represent ideal vectors for the delivery of therapeutic genes to vascular endothelial cells, as they are capable of infecting even slow or non-dividing cells and enable permanent transgene expression due to stable genome integration^{26,27}. Importantly, lentiviruses are already applied in clinical gene therapy²⁸. Our results show that insufficient targeting of the naked lentivirus can be overcome by combining lentiviral gene transfer with MMB-mediated targeting. Of note, MMB generated with negatively charged SO-Mag MNP were surprisingly well capable of binding the negatively charged lentiviruses. This may be explained by the finding that the SO-Mag MMB complex actually exhibited a positive ζ potential. This finding is particularly important regarding future generation of new MNP, as it demonstrates the system to be independent of the surface charge of the MNP itself. Thus, focus can primarily be put on

further improvement of magnetic properties. Our results strongly indicate that magnetic attraction of the lentiviral MMB towards the cell layer seems to be the main parameter determining the gene targeting efficiency of the method, as application of US alone did not increase the transduction efficiency to the same extent in our setting. US frequency and cycles per pulse have been shown to be of importance for improved MB gene delivery²⁹ determining the degree of MB rupture and induction of cell permeability and our chosen settings may not be optimal for MB dependent transduction under static conditions. Under flow conditions, however, application of US in combination with MF is necessary to achieve even higher transduction rates. In fact, only combined treatment resulted in successful gene delivery *in vivo*, as shown in a previous study by us using MMB coated with pDNA⁹. This is probably not only due to the resulting release of the cargo but also to the destruction of the MB itself, which prevents the further circulation and thus distribution of the MMB leading to its concentration at the target site. Furthermore, MB sonication has been found to induce caveolae- and clathrin-dependent endocytosis in targeted cells^{29,30} thereby promoting uptake of i.a. viral particles^{31,32}. Using our settings, we found transduction by lentiviral SO-Mag MMB to be mediated by caveolin-dependent endocytosis, potentially induced by sonication. We therefore hypothesize that the enhanced transduction efficiency of the MMB technique is the result of magnetic approximation between lentiviral MMB and cells and subsequent sonication-induced endocytosis.

The successful targeting of aortic endothelium by lentiviral SO-Mag MMB under flow conditions indicates the power of this targeting approach. Importantly, the potency to achieve physiologically relevant effects was confirmed by the successful delivery of human VEGF expressing lentivirus to mouse aortic endothelium under flow conditions *ex vivo*, which resulted in increased huVEGF expression and secretion as well as aortic vessel sprouting. Therapeutic angiogenesis by gene therapeutic approaches has been attempted in a variety of clinical phase I/II studies facilitating pDNA^{11,14,33} or adenoviral vectors^{34,35}, many of them with no or unsatisfactory results, potentially due to too low transgene expression³⁶. In addition, successful vector delivery was only achieved by direct tissue injection or local catheter-application of the genetic vectors^{13,36,37}. Therefore, an advanced intravascular targeting strategy, such as the lentiviral MMB technique, allowing for more efficient gene transfer, may constitute a valuable tool to achieve localized modulation of angiogenesis by targeted gene delivery

of VEGF. Indeed, our data demonstrate the great potential of this technique for gene therapeutic angiogenesis. Most importantly, we successfully confirmed the functionality of lentiviral MMB as a vascular gene delivery system *in vivo* achieving lentiviral transgene expression at the target site. To a significantly lesser extent, secondary sites of reporter gene expression were found in the lung and liver probably due to remnant MMB being filtered through these organs containing extensive vascular networks. These were also the sites of the highest MNP accumulation, which may partly explain the off-target expression. Of note, targeting of the dorsal skin with MF and US reduced non-specific transgene expression to the lung and liver in contrast to mice receiving only lentiviral MMB without MF and US treatment. These observations certainly highlight the great advantage with this technique in reducing non-specific side-effects upon systemic application, which is of clinical importance. To further reduce undesired lentiviral transgene expression in other organs, further optimization of the lentiviral MMB technique using for instance viral shielding, which has been proven effective in previous studies with adenoviruses³⁸, may be necessary. Most importantly though, this is the first time relevant lentiviral gene transfer via the systemic circulation was successfully accomplished using combined magnetic and ultrasound targeting. Thus, our study highlights the huge potential of the lentiviral MMB technique as a tool for gene therapy, with a wide application spectrum, and at the same time creates the foundation for future therapeutic applications.

Material and Methods

Antibodies and Chemicals

Rat PECAM-1 (#553370) was from BD Bioscience (Heidelberg, Germany). Alexa Fluor®555-labelled goat anti-rat antibody was from Life Technologies (Darmstadt, Germany). Collagenase A was from Roche (Mannheim, Germany). Luciferin was from Promega (Mannheim, Germany). All other chemicals were from Sigma-Aldrich (Taufkirchen, Germany).

Lentiviral constructs

Production of GFP-, luciferase- and huVEGF-expressing lentiviral particles has been described elsewhere³⁹. Non integrating fluorescent labeled lentiviral particles pCHIV.eGFP were generated as described by Lampe et al.⁴⁰. The physical viral titers (viral particles, VP) of lentiviral preparations were determined by reverse transcriptase activity measurements²⁵ and biological titers (infectious particles) were determined by

transduction of HEK293T cells and flow cytometry of transduced cells as described elsewhere³⁹.

Synthesis of magnetic nanoparticles

Synthesis of core-shell type iron oxide MNP has been described elsewhere²⁴. Surface modification protocols to generate PEI-Mag and SO-Mag MNP as well as further detailed characteristics of the used MNP have been described previously^{15,41}. Iron concentrations of the MNP suspensions were determined spectrophotometrically with o-phenantroline as described previously²⁴.

Preparation and characterization of magnetic microbubbles and coating with lentiviral particles

The phospholipid solution containing DPPE and DPPC (Lipoid) for production of magnetic microbubbles (MMB) was prepared as described elsewhere¹⁰. To generate a 150 and 250 µg Fe/ml MMB solutions, MNP (SO-Mag or PEI-Mag) corresponding to a total iron weight of 150 or 250 µg were added to 1 ml lipid solution in 1.5 ml glass vials with screw caps and silicon/PTFE membranes (Schubert & Weiss Omnilab GmbH, München, Germany). The mixtures were then covered with perfluorocarbon gas and shaken for 20s in a CapMix (3M ESPE, Seefeld, Germany). Lentiviral particles were added to the MMB solutions in an optimal VP:MNP²⁵. In detail, $3.3 \cdot 10^6$ VP/µg Fe, corresponding to $5 \cdot 10^8$ VP/ml MMB solution, were added and left to associate for 10 min before use. Unless otherwise stated, amounts of lentiviral MMB applied in different cell culture experiments were individually calculated to achieve a cell:VP ratio of 1:5. Size and density of MB in solution with or without associated MNP (SO-Mag or PEI-Mag) and lentivirus (pCHIV.eGFP) were measured in 1:1000 dilutions in Hank's balanced salt solution (HBSS; Biochrom, Berlin, Germany) using the Casy Counter (Schärfe Systems, Roche Diagnostics, Mannheim, Germany). From the resulting MMB concentrations (MB/ml) mean iron content (µg Fe/MMB) and MNP content (MNP/MMB) were calculated. ζ-potential of MMB in HBSS was measured by photon correlation spectroscopy using a Malvern 3000 HS Zetasizer (Malvern, Herrenberg, Germany). Magnetic moments were assessed by magnetic responsiveness measurements as described by Heidsieck⁴². Lentivirus binding was verified by flow cytometry analysis of pCHIV.eGFP-MMB using a FACS Canto II (BD Biosciences, Heidelberg, Germany). Magnetizability of MMB as well as lentivirus binding capacity was determined by exposing lentiviral MMB solutions to a magnetic field for 15 min and applying MMB-free supernatant as

well as MMB concentrates to endothelial cell culture. Culture plates were subsequently placed over a neodymium iron boron magnet (IBA Bio TAGnology, Goettingen, Germany) for 30 min and exposed to ultrasound (30 s, 1 MHz, 2 W/cm², 50% duty cycle) using an ultrasonic device from Rich-mar (G. Heinemann, Schwaebisch Gmuend, Germany). Cells were washed with PBS supplemented with calcium and provided with growth medium. GFP expression was detected 72 h later by fluorescence microscopy and flow cytometry.

Cell culture

Human umbilical vein endothelial cells (HUVEC) were purchased from PanBiotech (Aidenbach, Germany) and cultured in DMEM supplemented with 10% fetal calf serum, 1% Penicillin/Streptomycin and 50% complete EndoPAN3 medium (kit with 9 supplements; PanBiotech). All experiments with HUVEC were performed up to passage 5.

Application of the lentiviral MMB technique under static conditions

Medium on cells was exchanged by HBSS and lentiviral MMB corresponding to a multiplicity of infection of 5 were added. Lentiviral MMB were attracted to the bottom by placing the culture plate on top of a neodymium iron boron magnet and subsequent sonication (30 s, 1 MHz, 2 W/cm², 50% duty cycle). Single method parameters (MMB, US, MF) were omitted to assess their contribution to the whole technique, otherwise the procedure was kept the same. To assess the endocytic mechanism relevant for lentiviral MMB-mediated gene delivery, HUVEC were treated with specific inhibitors (30 min) previous to SO-Mag MMB mediated transduction. Caveolae-mediated endocytosis was inhibited by incubation with 10 mM methyl- β -cyclodextrin (M β CD). Inhibition of phagosome-lysosome fusion was accomplished by incubation with 10 nM ammoniumchloride (NH₄Cl) and 10 μ M Cytochalasin B (CytoB) were used to inhibit the clathrin-mediated endocytic pathway. After lentiviral MMB treatment, cells were further incubated on the magnet for 30 min at 37°C. Cells were then rinsed with PBS supplemented with calcium and cultured in complete growth medium for another 72 h. GFP expression was assessed by fluorescence microscopy and flow cytometry.

Application of the lentiviral MMB technique under flow *in vitro*

HUVEC were grown to confluence on IBIDI μ -slides IV^{0.4} (Martinsried, Germany) and perfused

with HBSS at shear rates of 1, 5 or 7.5 dyn/cm² using a syringe pump (kdScientific, Holliston, MA, USA). 20 μ l of MMB or lipid-MNP mixture were preincubated with a luciferase-expressing lentivirus for 10 min, diluted 1:10 in HBSS and injected into the system. If indicated, US (30 s, 1 MHz, 2 W/cm², 50% duty cycle) and MF were simultaneously applied to the cells. After further 2 min MF exposure under continued perfusion cells were incubated in complete growth medium for 72 h. Luciferase expression was assessed by application of 0.5 mg/ml luciferin using an IVIS imaging system from PerkinElmer (Waltham, MA, USA). Transduction efficiencies were quantified by measurement of pixel density using the Hokawo software (Hamamatsu Photonics, Hamamatsu City, Japan).

Application of the lentiviral MMB technique under flow in isolated mouse aortas

C57BL/6J wild type mice (Charles River, Burlington, MA, USA) were euthanized by cervical dislocation under anaesthesia (Midazolam 5 mg/kg; Medetomidin 0.5 mg/kg; Fentanyl 0.05 mg/kg). Thoracic aortas were isolated and intercostal arteries were cauterized to prevent leakage. Aortas were bilaterally catheterized and mounted above a magnet in a recirculation system constructed for MMB-mediated transduction (see Fig. 3e). Aortas (diameter ~1 mm) were perfused with serum-free DMEM at around 7-8 dyn/cm². 200 μ l of LV-MMB (corresponding to 9.9*10⁷ VP) were diluted 1:5 in HBSS and were slowly injected into the plastic tube upstream of the perfused aorta. US (120 s, 1 MHz, 2 W/cm², 50% duty cycle) was applied simultaneously at the site of magnetic field application. After further 30 min of perfusion and MF exposure aortas were transferred to a cell culture dish with 5 ml of DMEM supplemented with 20% FCS and left for gene expression for 6 days in a humidified incubator before assaying. Aortic ring sprouting assays were performed as previously described⁴³.

Immunofluorescence staining of mouse aortas

To assess localized transgene delivery by LV-MMB, GFP expression in whole mouse aortas was visualized by fluorescence microscopy. For immunofluorescence staining aortas were fixed for 1 h in 2% PFA, left in 20% sucrose over-night, embedded in OCT, and frozen at -80°C. Five μ m cross-sectional slices were cut with a cryotome, blocked for 30 min with 5% BSA in PBS-T (0.1% Tween-20), and incubated with anti-PECAM-1 antibody (1:100 dilution in PBS-T supplemented with 1% BSA) overnight. Sections were washed thrice with PBS-T and secondary antibody (1:500 dilution in PBS-T

supplemented with 1% BSA) was incubated for 2 h. After another three washing steps, the sections were incubated with Hoechst nuclear stain (50 µg/ml in PBS). The sections were then washed once more, and mounted under a coverslip. Fluorescence pictures were taken at 20-fold magnification (Leica DMI4000B, Leica Microsystems, Wetzlar, Germany).

RNA isolation from mouse aortas and qRT-PCR

Aortas transduced with huVEGF or GFP lentivirus-coated MMB were cultured in DMEM supplemented with 10% fetal calf serum, 1% penicillin/streptomycin and 50% complete EndoPAN3 medium for 24 h. Tissues were then mechanically ground in RNA lysis buffer and total RNA was isolated using the peqGOLD total RNA Kit (Peqlab). Quantitative reverse-transcriptase PCR (qRT-PCR) was performed using the TaqMan real-time PCR system (Applied Biosystems) as described before⁴⁴. Primers and probes for human VEGF (fw: GCCTTGCTGCTCTACCTCCAC; rv: ATGATTCTGCCCTCCTCTTCT; probe: AAGTGGTCCCAGGCTGCACCCAT, FAM) and murine 18S rRNA, as house-keeping gene, (NCBI Ref.Seq. X03205.1; #4310893E) were purchased from Applied Biosystems.

Application of the lentiviral MMB technique *in vivo*

All animal experiments were performed in accordance with the German animal protection law and approved by the district government of upper Bavaria (Regierung von Oberbayern, approval reference number AZ55.2-1-54-2532-36-2015). The study corresponds to the *Guide for the Care and Use of Laboratory Animals* published by the US National Institutes of Health (NIH Publication No. 85-23, revised 1996). All surgical procedures were performed under deep anaesthesia achieved by i.p. injection of Midazolam (5 mg/kg body weight), Medetomidin (0.5 mg/kg body weight) and Fentanyl (0.05 mg/kg body weight) in 0.9% NaCl. The implantation of the dorsal skinfold chamber (DSFC) in 16-24 week old C57BL/6J mice (Charles River, Sulzfeld, Germany) was performed as described before⁴⁵. The Arteria carotis of anaesthetized mice was catheterized the following day⁴⁵ and 100 µl of lentiviral MMB (250 µg Fe/ml; 8.3×10^7 VP/ml) were slowly injected with simultaneous application of a MF using an electromagnet (5min, 1.039 T) and US (30s, 2 W/cm², 1 MHz, 50% duty cycle) from both sides of the DSFC window (see figure 5a). Afterwards, the catheter was removed and the skin incision was closed by suture. Anaesthesia was antagonized by s.c.

injection of Flumazenil (0.5 mg/kg body weight) and Atipamezol (2.5 mg/kg body weight) in 0.9 % NaCl and postsurgical analgesia was provided by s.c. injection of 0.065 mg/kg body weight Buprenorphin with the first injection 10 min before injection of the antagonisation following administration in a 12 hour-cycle until 3 days after lentiviral MMB application.

Bioluminescence imaging

To assess the systemic distribution of luciferase transgene expression resulting from lentiviral MMB transduction, luciferase activity was analysed 8 days after treatment. Mice were anaesthetized and luciferin was applied i.p. (100 µl, 3 mg/ml in 0.9% NaCl). Bioluminescence was detected using an IVIS imaging system from PerkinElmer (Waltham, MA, USA).

DNA isolation from mouse tissue and quantification of proviral genome copy numbers

Genomic DNA was extracted from mechanically homogenized tissues (dorsal skin tissue, livers and lungs) of mice receiving lentiviral MMB with or without MF and US targeting using the NucleoSpin® Tissue gDNA Kit (Macherey-Nagel). Provirus genome copy numbers per cell were assessed using the Lenti-X™ Provirus Quantitation Kit (Macherey-Nagel) following the manufacturer's instructions.

Detection of magnetic nanoparticles amounts in organs

To determine the systemic distribution of MNP in lentiviral MMB treated mice, organs were isolated using non-metallic (iron-free) instruments, mechanically homogenized in PBS and exposed to magnetic particle spectroscopy (MPS) as described before⁴⁶.

Statistical analysis

All data are presented as means ± SEM. All statistical analyses were performed using Sigma Plot version 10.0. For multiple comparisons of normal distributed data the one-way analysis of variance (1-way ANOVA), followed by Student Newman-Keuls post-hoc test was performed. Differences were considered significant at an error probability level of $p \leq 0.05$.

Abbreviations

CytoB: cytochalasin B; DSFC: dorsal skinfold chamber; GFP: green fluorescent protein; LV: lentivirus; MB: microbubbles; MβCD: methyl-β-cyclodextrin; MF: magnetic field; MMB: magnetic microbubbles; MNP: magnetic

nanoparticles; US: ultrasound; VEGF: vascular endothelial growth factor.

Acknowledgement

This work was supported by the German Research Foundation (DFG) within the Research Unit 917.

Conflict of Interest

The authors have declared that no conflict of interest exists.

References

- Feinstein S B. The powerful microbubble: from bench to bedside, from intravascular indicator to therapeutic delivery system, and beyond. *Am J Physiol Heart Circ Physiol.* 2004; 287: H450-7.
- Lindner J R and Kaul S. Delivery of drugs with ultrasound. *Echocardiography.* 2001; 18: 329-37.
- Bekeredjian R, Grayburn P A and Shohet R V. Use of ultrasound contrast agents for gene or drug delivery in cardiovascular medicine. *J Am Coll Cardiol.* 2005; 45: 329-35.
- Qin S, Caskey C F and Ferrara K W. Ultrasound contrast microbubbles in imaging and therapy: physical principles and engineering. *Phys Med Biol.* 2009; 54: R27-57.
- Lammers T, Kiessling F, Hennink W E, et al. Drug targeting to tumors: principles, pitfalls and (pre-) clinical progress. *J Control Release.* 2012; 161: 175-87.
- Webster D M, Sundaram P and Byrne M E. Injectable nanomaterials for drug delivery: carriers, targeting moieties, and therapeutics. *Eur J Pharm Biopharm.* 2013; 84: 1-20.
- Krotz F, de Wit C, Sohn H Y, et al. Magnetofection—a highly efficient tool for antisense oligonucleotide delivery in vitro and in vivo. *Mol Ther.* 2003; 7: 700-10.
- Krotz F, Sohn H Y, Gloe T, et al. Magnetofection potentiates gene delivery to cultured endothelial cells. *J Vasc Res.* 2003; 40: 425-34.
- Mannell H, Pircher J, Fochler F, et al. Site directed vascular gene delivery in vivo by ultrasonic destruction of magnetic nanoparticle coated microbubbles. *Nanomedicine.* 2012; 8: 1309-18.
- Mannell H, Pircher J, Rathel T, et al. Targeted endothelial gene delivery by ultrasonic destruction of magnetic microbubbles carrying lentiviral vectors. *Pharm Res.* 2012; 29: 1282-94.
- Ferrara N, Gerber H P and LeCouter J. The biology of VEGF and its receptors. *Nat Med.* 2003; 9: 669-76.
- Grochot-Przeczek A, Dulak J and Jozkowicz A. Therapeutic angiogenesis for revascularization in peripheral artery disease. *Gene.* 2013; 525: 220-8.
- Yla-Herttuala S. Cardiovascular gene therapy with vascular endothelial growth factors. *Gene.* 2013; 525: 217-9.
- Ellis L M and Hicklin D J. VEGF-targeted therapy: mechanisms of anti-tumour activity. *Nat Rev Cancer.* 2008; 8: 579-91.
- Almstatter I, Mykhaylyk O, Settles M, et al. Characterization of magnetic viral complexes for targeted delivery in oncology. *Theranostics.* 2015; 5: 667-85.
- Hussain K M, Leong K L, Ng M M, et al. The essential role of clathrin-mediated endocytosis in the infectious entry of human enterovirus 71. *J Biol Chem.* 2011; 286: 309-21.
- Rodal S K, Skretting G, Garred O, et al. Extraction of cholesterol with methyl-beta-cyclodextrin perturbs formation of clathrin-coated endocytic vesicles. *Mol Biol Cell.* 1999; 10: 961-74.
- Hart P D and Young M R. Ammonium chloride, an inhibitor of phagosome-lysosome fusion in macrophages, concurrently induces phagosome-endosome fusion, and opens a novel pathway: studies of a pathogenic mycobacterium and a nonpathogenic yeast. *J Exp Med.* 1991; 174: 881-9.
- Menger M D, Laschke M W and Vollmar B. Viewing the microcirculation through the window: some twenty years experience with the hamster dorsal skinfold chamber. *Eur Surg Res.* 2002; 34: 83-91.
- Mou X, Ali Z, Li S, et al. Applications of Magnetic Nanoparticles in Targeted Drug Delivery System. *J Nanosci Nanotechnol.* 2015; 15: 54-62.
- Laurent S, Saei A A, Behzadi S, et al. Superparamagnetic iron oxide nanoparticles for delivery of therapeutic agents: opportunities and challenges. *Expert Opin Drug Deliv.* 2014; 11: 1449-70.
- Mannell H, Hammitzsch A, Mettler R, et al. Suppression of DNA-PKcs enhances FGF-2 dependent human endothelial cell proliferation via negative regulation of Akt. *Cell Signal.* 2010; 22: 88-96.
- Vosen S, Rieck S, Heidsieck A, et al. Vascular Repair by Circumferential Cell Therapy Using Magnetic Nanoparticles and Tailored Magnets. *ACS Nano.* 2016; 10: 369-76.
- Mykhaylyk O, Antequera Y S, Vlaskou D, et al. Generation of magnetic nonviral gene transfer agents and magnetofection in vitro. *Nat Protoc.* 2007; 2: 2391-411.
- Trueck C, Zimmermann K, Mykhaylyk O, et al. Optimization of magnetic nanoparticle-assisted lentiviral gene transfer. *Pharm Res.* 2012; 29: 1255-69.
- Buchschacher G L, Jr. and Wong-Staal F. Development of lentiviral vectors for gene therapy for human diseases. *Blood.* 2000; 95: 2499-504.
- Vigna E and Naldini L. Lentiviral vectors: excellent tools for experimental gene transfer and promising candidates for gene therapy. *J Gene Med.* 2000; 2: 308-16.
- Kotterman M A, Chalberg T W and Schaffer D V. Viral Vectors for Gene Therapy: Translational and Clinical Outlook. *Annu Rev Biomed Eng.* 2015; 17: 63-89.
- Meijering B D, Juffermans L J, van Wamel A, et al. Ultrasound and microbubble-targeted delivery of macromolecules is regulated by induction of endocytosis and pore formation. *Circ Res.* 2009; 104: 679-87.
- Afadzi M, Strand S P, Nilssen E A, et al. Mechanisms of the ultrasound-mediated intracellular delivery of liposomes and dextrans. *IEEE Trans Ultrason Ferroelectr Freq Control.* 2013; 60: 21-33.
- Sorace A G, Warram J M, Mahoney M, et al. Enhancement of adenovirus delivery after ultrasound-stimulated therapy in a cancer model. *Ultrasound Med Biol.* 2013; 39: 2374-81.
- Jin L F, Li F, Wang H P, et al. Ultrasound targeted microbubble destruction stimulates cellular endocytosis in facilitation of adeno-associated virus delivery. *Int J Mol Sci.* 2013; 14: 9737-50.
- Stewart D J, Kutryk M J, Fitchett D, et al. VEGF gene therapy fails to improve perfusion of ischemic myocardium in patients with advanced coronary disease: results of the NORTHERN trial. *Mol Ther.* 2009; 17: 1109-15.
- Rajagopalan S, Mohler E, 3rd, Lederman R J, et al. Regional Angiogenesis with Vascular Endothelial Growth Factor (VEGF) in peripheral arterial disease: Design of the RAVE trial. *Am Heart J.* 2003; 145: 1114-8.
- Stewart D J, Hilton J D, Arnold J M, et al. Angiogenic gene therapy in patients with nonrevascularizable ischemic heart disease: a phase 2 randomized, controlled trial of AdVEGF(121) (AdVEGF121) versus maximum medical treatment. *Gene Ther.* 2006; 13: 1503-11.
- Giacca M and Zaccagna S. Virus-mediated gene delivery for human gene therapy. *J Control Release.* 2012; 161: 377-88.
- Makinen K, Manninen H, Hedman M, et al. Increased vascularity detected by digital subtraction angiography after VEGF gene transfer to human lower limb artery: a randomized, placebo-controlled, double-blinded phase II study. *Mol Ther.* 2002; 6: 127-33.
- Kreppel F and Kochanek S. Modification of adenovirus gene transfer vectors with synthetic polymers: a scientific review and technical guide. *Mol Ther.* 2008; 16: 16-29.
- Hofmann A, Wenzel D, Becher U M, et al. Combined targeting of lentiviral vectors and positioning of transduced cells by magnetic nanoparticles. *Proc Natl Acad Sci U S A.* 2009; 106: 44-9.
- Lampe M, Briggs J A, Endress T, et al. Double-labelled HIV-1 particles for study of virus-cell interaction. *Virology.* 2007; 360: 92-104.
- Mykhaylyk O, Sobisch T, Almstatter I, et al. Silica-iron oxide magnetic nanoparticles modified for gene delivery: a search for optimum and quantitative criteria. *Pharm Res.* 2012; 29: 1344-65.
- Heidsieck A. Simple Two-Dimensional Object Tracking based on a Graph Algorithm. *arXiv:1412.1216.* 2014.
- Mannell H, Hellwig N, Gloe T, et al. Inhibition of the tyrosine phosphatase SHP-2 suppresses angiogenesis in vitro and in vivo. *J Vasc Res.* 2008; 45: 153-63.
- Wornle M, Schmid H, Banas B, et al. Novel role of toll-like receptor 3 in hepatitis C-associated glomerulonephritis. *Am J Pathol.* 2006; 168: 370-85.
- Pircher J, Fochler F, Czermak T, et al. Hydrogen sulfide-releasing aspirin derivative ACS14 exerts strong antithrombotic effects in vitro and in vivo. *Arterioscler Thromb Vasc Biol.* 2012; 32: 2884-91.
- Wenzel D, Rieck S, Vosen S, et al. Identification of magnetic nanoparticles for combined positioning and lentiviral transduction of endothelial cells. *Pharm Res.* 2012; 29: 1242-54.